# Template-Induced and Molecular Recognition Directed Hierarchical Generation of Supramolecular Assemblies from Molecular Strands

**Volker Berl,[a, b] Michael J. Krische,[a, c] Ivan Huc,[a, d] Jean-Marie Lehn,*[a] and Marc Schmutz[e]**

**Abstract:** The linear oligo-isophthalamide strand **1** undergoes a conformational reorganization upon binding of a cyanuric acid template as effector to afford a helical disklike object possessing radially disposed alkyl residues. Solvophobic and stacking interactions, in turn, drive a "second level" self-assembly of the templated structure, the stacking of the helical disks, to yield fibers as revealed by electron microscopy. These data provide insight into the interplay of the different structural and interactional features of the molecular components towards the formation of supramolecular fibers through sequential hierarchical self-assembly events and suggest design strategies for the effector-controlled generation of related supramolecular assemblies.

**Keywords:** fibers · helicity · hydrogen bonding · self-assembly · supramolecular chemistry

## Introduction

Recognition processes occurring at the molecular level may lead to changes at the level of the material, thus expressing molecular information on the macroscopic scale. They may operate both in the formation of supramolecular materials[1] from their components and in the induction of novel properties through specific interactions. The generation of supramolecular materials offers the advantage over both stepwise "bottom-up" strategies and "top-down" methods of fabrication[2] to give access to nanosize entities of more or less well-defined structure by recognition-controlled self-assembly from selected components connected through specific interactions of organic or inorganic nature.[3–5] For example, in the specific case of H-bonded systems, the determination of persistent structural motifs[6, 7] has allowed their integration into the design of programmed molecular components for the self-assembly of discrete[8] and polymeric[9] supramolecular liquid crystals, conductive fibers,[10] and organic solids possessing magnetic properties.[11] A step beyond concerns the investigation of sequential and hierarchical self-organization events in which a given step sets the stage for a subsequent one. Thus, internally enforced molecular helices[12] may self-assemble to form extended fibers,[13] and molecular disks resulting from the assembly of three sector molecules through hydrogen bonding thereafter stack to yield discotic liquid crystals.[14] Three levels of sequential assembly may even be distinguished in the generation of supramolecular liquid crystalline polymers[9a,b] resulting from the initial formation of a supramolecular strand, followed by the assembly of three strands into columns which subsequently associate into fibers. In the present work, an initial H-bond mediated recognition event leads to the effector-induced generation of a coiled object which, in turn, undergoes self-assembly into a columnar entity, resulting in the formation of polymeric fibers. The initial H-bond mediated substrate – receptor interaction may also be viewed as the deconvolution of a virtual dynamic library[15] of conformers to give a discrete supramolecular object which promotes a subsequent or "second level" self-assembly event.

Within the general context of programmed chemical systems,[3] this amounts to the reading of molecular information through a specific interactional algorithm to yield a

[a] Prof. Dr. J.-M. Lehn, V. Berl, Dr. M. J. Krische, Dr. I. Huc
Laboratoire de Chimie Supramoléculaire, ESA 7006 of the CNRS, ISIS, Université Louis Pasteur, 4 rue Blaise Pascal
67000 Strasbourg (France)
Fax: (+33) 388 411020
E-mail: lehn@chimie.u-strasbg.fr

[b] V. Berl
Affiliated institution: Forschungszentrum Karlsruhe GmbH
Institut für Nanotechnologie, Postfach 3640
76021 Karlsruhe (Germany)

[c] Dr. M. J. Krische
Present address: University of Texas at Austin
Department of Chemistry and Biochemistry, Austin, TX 78712 (USA)

[d] Dr. I. Huc
Present address: Institut Européen de Chimie et Biologie, ENSCPB, Av. Pey Berland, 33402 Talence Cedex (France)

[e] Dr. M. Schmutz
Institut de Génétique et de Biologie Moléculaire et Cellulaire, CNRS/INSERM/ULP, BP 163, C.U. de Strasbourg, 67404 Illkirch (France)



0947-6539/00/0611-1938 $ 17.50+.50/0

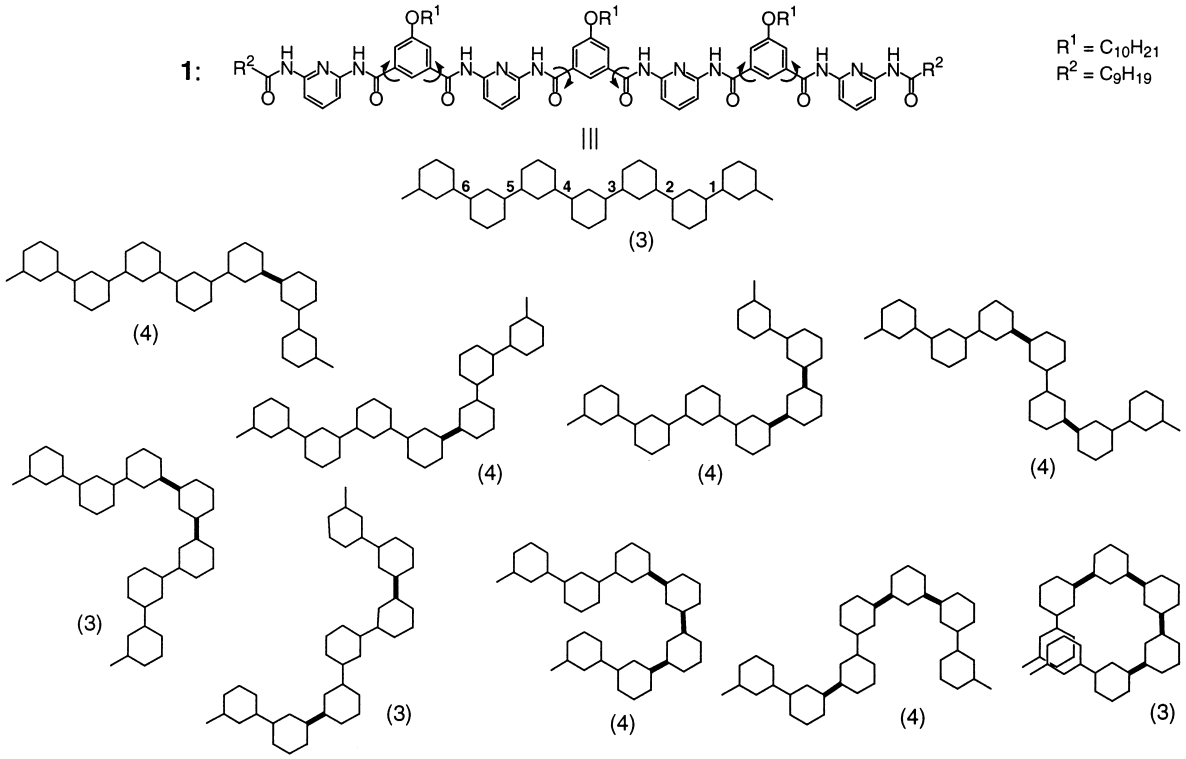


Figure 1. Possible rotameric forms of the molecular strand **1**. The linkages between the hexagons represent the CO–NH fragments. The thick linkages indicate those within which 180° rotation was performed around the CO–aromatic ring bond. Ten rotamers are represented corresponding to the combinations obtained by rotations within linkages 2 to 5. The number in parentheses below each structure gives the number of different combinations obtained by 180° rotation about linkages 1 and 6, resulting in 36 different rotamers.

defined structural output. Such was also the case in the formation of inorganic double helices[16] and of double subroutine architectures,[18a] induced by the binding of metal ions of defined coordination geometry to suitably designed ligands. It was furthermore shown in the case of the self-assembly of double helicates[17] and of a double subroutine architecture[18b, 18c] that the reading of the same ligand information with different sets of metal ions yields different inorganic architectures as outputs.[16, 17, 18b] This is of particular interest, since it indicates that the information contained in a molecular entity does not necessarily code for a single species only, but may generate different outputs depending on how it is read out and processed.

**Abstract in French:** *Le brin linéaire oligo-isophthalamide **1** subit une réorganisation conformationnelle lorsqu'il lie un dérivé de l'acide cyanurique servant d'effecteur pour la formation d'un objet discoïde présentant des groupes alkyles disposés radialement. Des interactions solvophobes et d'empilement induisent à leur tour un autoassemblage de ces disques hélicoïdaux en fibres, mises en évidence par microscopie électronique. Ces données permettent d'analyser les divers facteurs structuraux et interactionnels qui conduisent à la formation de fibres supramoléculaires par un processus d'autoassemblage séquentiel hiérarchisé. Elles suggèrent aussi des stratégies pour la génération contrôlée d'assemblées supramoléculaires de types donnés à l'aide d'effecteurs spécifiques.*

## Results and Discussion

**Design strategy**: A given linear sequence of H-bond donor(D)/acceptor(A) arrays may adopt different geometries upon interaction with different complementary templates, exemplifying that the information manifested in the arrays may be expressed differently depending on how it is read through a given interactional algorithm. In the case of the conformationally dynamic receptor **1** containing a linear sequence of four DAD H-bonding subunits, a dynamic library of 36 different quasi-planar/conjugated rotamers is obtained, if one considers only rotation about aryl–CO bonds (Figure 1). These 36 species have occurrences of 1 or 2 depending on their symmetry. Their energies and therefore the population of each conformer may differ due to long-range effects.

The outcome of a selection within this library through binding of an effector depends on the template employed for deconvolution. With an ADA imide template, one would expect a linear readout of the strand to give a mixture of many different conformers of the supramolecular entity thus formed (Figure 2, bottom). In contrast, upon the binding of a double-faced, Janus type, ADA/ADA cyanurate template,[19] curvature is introduced into the backbone of the receptor **1**, so that binding of two effector units may generate three conformers of C, S, and helical shape (Figure 2, top). Consequently, selection from the dynamic library of possible conformational isomers of **1** occurs differentially as a function of how the receptor is read.

A possible outcome of the interaction of strand **1** with the monosubstituted cyanurate **4** is a helical disklike object **1:4**$_2$,

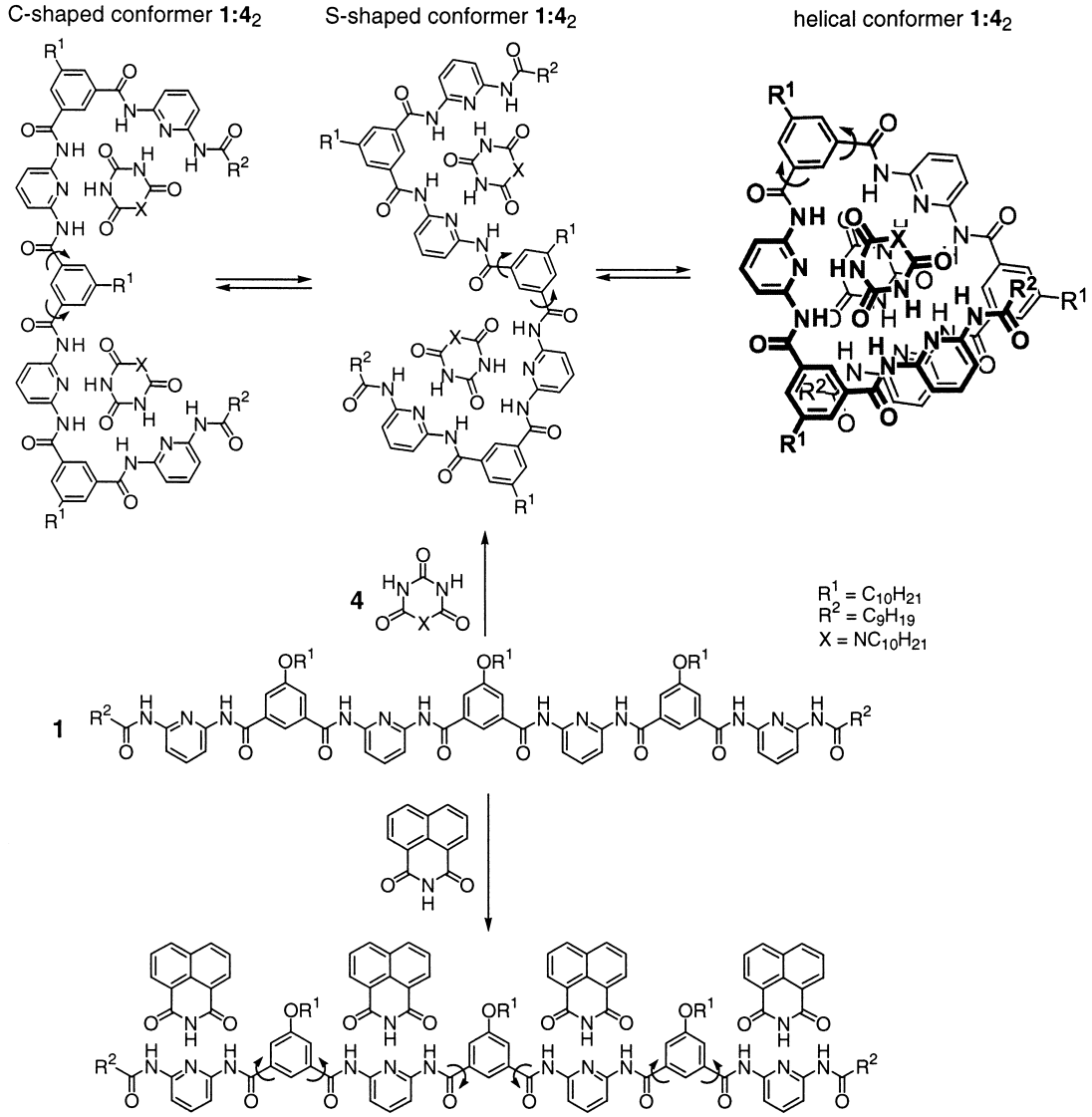


Figure 2. Template-dependent expression of the information stored in receptor **1** as a function of the interaction/recognition algorithm of the effector. The helical form (right) has been slightly enlarged for clarity.

in which two units of **4** bind internally to a single strand of **1** to give a discrete coiled, closed helical entity (Figure 2, top right, and CH, Figure 3). The 5-substitution of the isophthaloyl moieties by a long-chain *n*-alkoxy group introduces radially protruding alkyl residues. Molecular modeling calculations[20] support this assumption and show the coiling of the ligand around the cyanurate template (Figure 4). As is also the case for the columnar self-assembly of helicene derivatives possessing peripherally disposed alkyl groups,[21] the primary product, (**1:4**$_2$)CH, may undergo a subsequent self-assembly process to form helical columns (**1:4**$_2$)$_n$ (CHC, Figure 3). This "second level" self-assembly event is equivalent to the generation of discotic supramolecular entities and is presumably driven by Van der Waals stacking interactions, as well as possible polar and medium (solvophobic) effects. In addition to the above discrete coiled species (**1:4**$_2$)CH, the cyanurate template **4** could bind to receptor **1** in a frame shifted manner in which adjacent receptors **1** share a cyanurate template, giving either a bridged helical unit (BH, Figure 3) or two types of non-helical bridged forms, linear (BLF) or bent (BBF, Figure 3); the former thereafter may assemble into a helical supramolecular columnar entity (BHC).

**Synthesis of the molecular components**: For the synthesis of the oligoisophthalamide **1**, we searched for a modular and convergent route amenable to the preparation of gram quantities and permitting facile preparation of a variety of structural derivatives. Thus, dimethyl 5-hydroxyisophthalate was O-alkylated with decyl bromide to give diester **2a**. Exposure of **2a** to excess 2,6-diaminopyridine monolithium salt yields diamine **3a**. Subsequent mono-acylation provides the mono-amine mono-amide **3b**, which upon treatment with isophthaloyl chloride **2c** smoothly affords the oligo-isophthalamide **1**. Decyl cyanurate **4** was obtained by the direct N-alkylation of cyanuric acid with decyl bromide (Scheme 1).

**First level structuration, formation of helical segments**: The $^1$H NMR spectra of the highly soluble isophthalamide **1** feature broadened aromatic and aliphatic signals. This is likely due to nonspecific intermolecular associations involving the



0947-6539/00/0611-1940 $ 17.50+.50/0 *Chem. Eur. J.* **2000**, *6*, No. 11

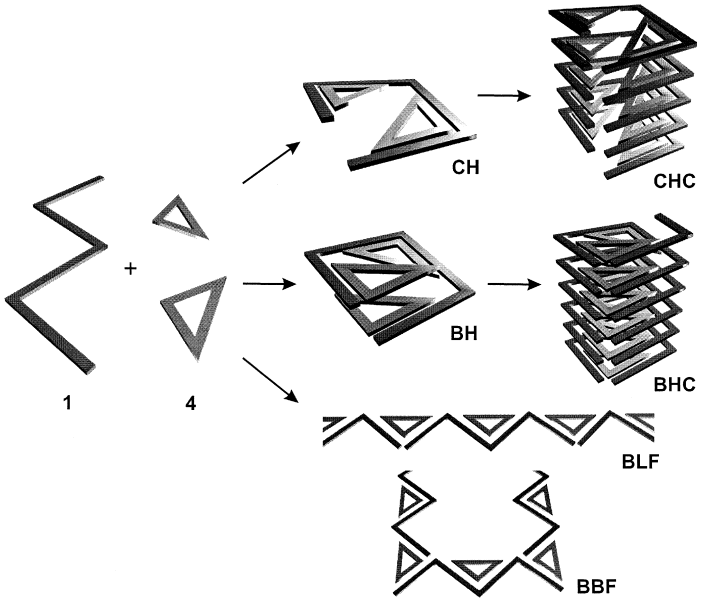


Figure 3. Hierarchical self-assembly process enforced by effector binding followed by aggregation into helical columns or linear "wavy" strands. The alternative binding modes of oligoamide **1** with the cyanurate template **4** generate units of composition **1:4**$_2$ which may adopt several forms: an internally bound, closed helical form (CH), a bridged helical form (BH), or two types of non-helical bridged forms, linear (BLF) or bent (BBF). CH and BH may assemble into helical columns CHC and BHC, respectively.

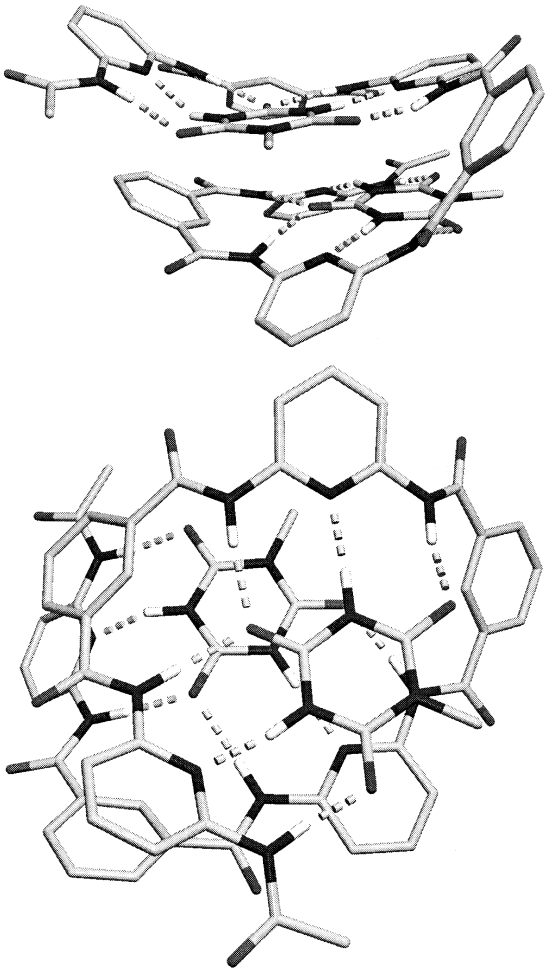

Figure 4. Computer-minimized structure of the **1:4**$_2$ supermolecule. Top: side view. Bottom: top view.

numerous hydrogen-bond acceptors and donors and to conformational diversity due to a variety of possible rotameric forms. Although significant sharpening of the spectra takes place upon addition of 5% $CD_3OD$ which competes with the various H-bonding sites, or upon dilution of the sample which disfavors intermolecular association, the $^1$H NMR spectrum of **1** in $CDCl_3$ at 0.5 mM still displays broad signals. (Figure 5a).

Remarkable sharpening of the signals occurs upon incremental introduction of up to two equivalents of cyanurate **4** to a solution of **1** in $CDCl_3$. This, along with a downfield shift of the amide-hydrogen signals, indicates the formation of a discrete species upon binding of **4** (Figure 5c). Apparently, specific association between **1** and cyanurate **4** resolves the ill-defined mixture of aggregates and conformers formed by **1** alone.

Adding at the same concentration (0.5 mM) four equivalents of the simple ADA naphthalimide template (Figure 2) has very little effect on the shape $^1$H NMR spectrum, which still displays broad peaks, even upon concentration to 10 mM, intended to compensate for the presumably much weak-

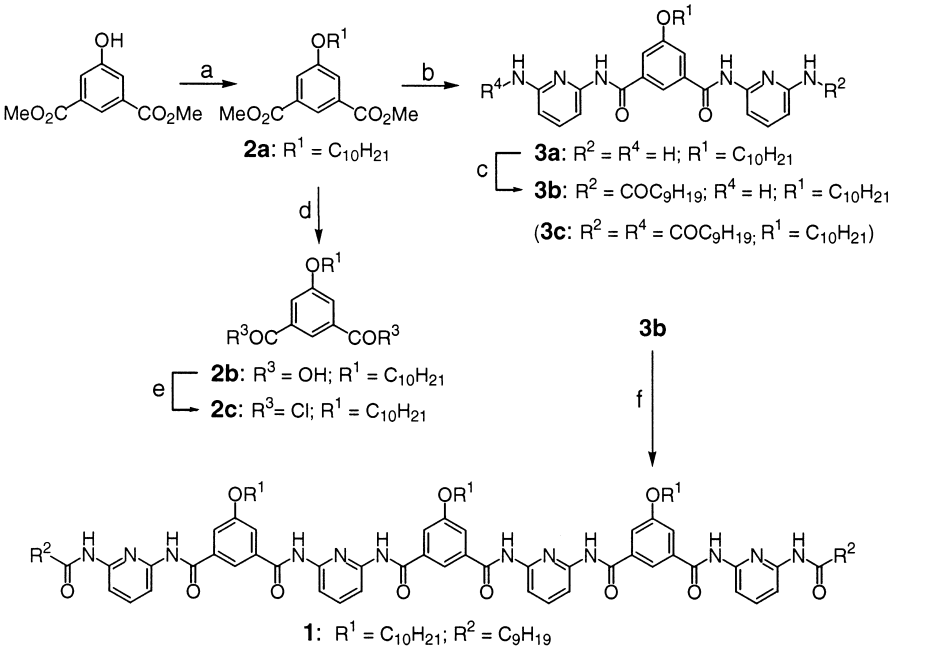


Scheme 1. Synthesis of the oligoisophthalamide **1**. a) $BrC_{10}H_{21}$, DMF, $K_2CO_3$, room temperature; b) 2,6-diaminopyridine, BuLi, THF, −78 °C; c) $C_9H_{19}COCl$, $NEt_3$, THF, 0 °C; d) EtOH, aq. NaOH; e) $SOCl_2$, reflux; f) **2c**, $NEt_3$, THF, 0 °C.

  0947-6539/00/0611-1941 $ 17.50+.50/0 

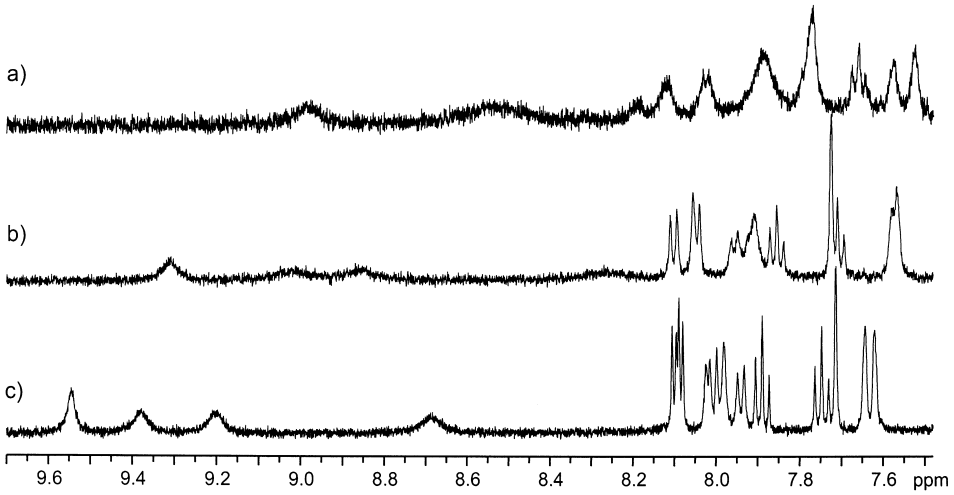


Figure 5. 500 MHz $^1$H-NMR spectra of **1** at a concentration of 0.5 mM in $CDCl_3$. a) 0 equiv of **4**; b) 1 equiv of **4**; c) 2 equiv of **4**.

addition of **4** to **1** (0.5 mM) in $CDCl_3$ (Figure 7a). The calculated values of log $Ka_1 = 3.9(0.2)$ and log $Ka_2 = 8.2(0.1)$ are of the same order of magnitude as those obtained for similar systems[19] and, in fact, indicate a positive cooperative effect for the binding of the second cyanurate guest. Indeed, when the region between 0 and 2 equivalents of added cyanurate is expanded (Figure 7b), an inflection point at 1 equivalent of added cyanurate is observed, which also supports a weak positive cooperativity. This could be due to a

er binding constant displayed by this system. These results suggest that the imide template interacts with the molecular strand in a different way and that whatever entity may be formed, it is different from that obtained with cyanurate **4**.

That a species **1:4**$_2$ of 1:2 binding stoichiometry had indeed formed was confirmed by applying Job's method of continuous variation to NMR results for species in rapid exchange.[22] The chemical shifts of the amide hydrogens were monitored, and the product of the mole fraction of **1** $X(\mathbf{1})$ by $\Delta(\delta)$, the observed chemical shifts minus the chemical shifts of free **1**, was plotted as a function of $X(\mathbf{1})$ (Figure 6).

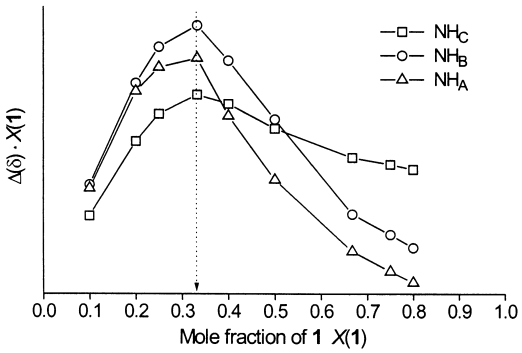


Figure 6. Determination of the 1:2 binding stoichiometry by a Job plot of the system **1:4** at constant total concentration of 2.0 mM; the product of the mole fraction of **1** $X(\mathbf{1})$ by $\Delta(\delta)$, the observed chemical shifts minus the chemical shifts of free **1**, is plotted as a function of $X(\mathbf{1})$. The *y* axes have been normalized.

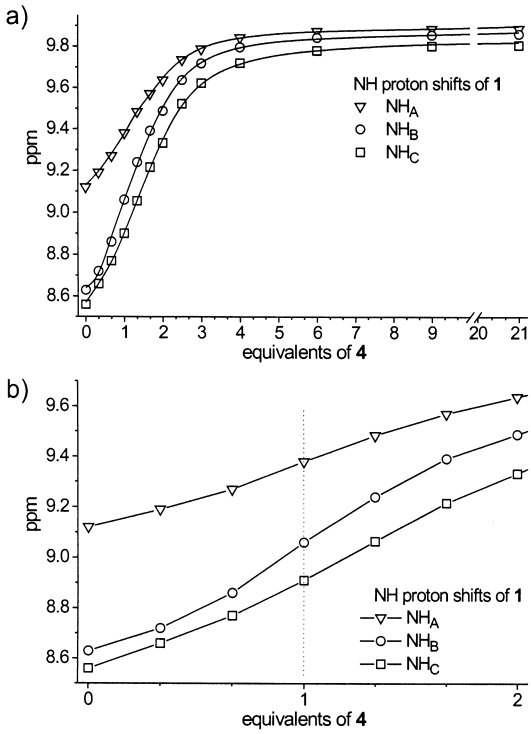


Figure 7. $^1$H NMR titration plot of the chemical shift values of three of the four NH protons of **1** ($c_0 = 0.5$ mM) as a function of added equivalents of cyanurate **4**. The straight lines represent the calculated fitting curves for the experimental data point series.

Additionally, association constants for the binding of cyanurate were determined using the Chem-Equili program.[23] The calculations were based on the assumption of two solution-state equilibria [Eqs. (1) and (2)].

$$Ka_1: (\mathbf{1}) + (\mathbf{4}) \rightleftharpoons (\mathbf{1{:}4}) \quad (1)$$

$$Ka_2: (\mathbf{1}) + 2(\mathbf{4}) \rightleftharpoons (\mathbf{1{:}4_2}) \quad (2)$$

Data sets were obtained by the analysis of the $^1$H NMR titration curves for the NH protons, obtained by progressive preorganization of the strand by the first molecule of cyanurate, facilitating the binding of the second one. To further corroborate these association constants, a dilution experiment (vide supra) was conducted in which the decreasing chemical shifts of the NH proton signals were used as data input for the Chem-Equili analysis. The calculated values, though presenting a greater margin of error, confirm the validity of those previously obtained: log $Ka_1 = 3.8(2.5)$ and log $Ka_2 = 8.4(1.5)$ (Figure 8).

$^1$H NOE experiments proved particularly diagnostic for the characterization of the helical geometry of the **1:4**$_2$ entity,



0947-6539/00/0611-1942 $ 17.50+.50/0 *Chem. Eur. J.* **2000**, *6*, No. 11

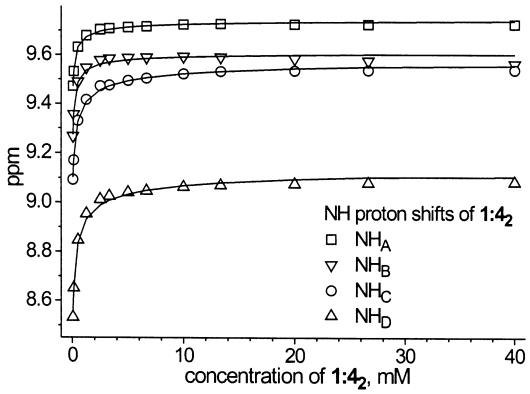


Figure 8. Dilution study of the **1:4**$_2$ supermolecule in $CDCl_3$. The data series represent the chemical shift variation for the NH proton NMR signals of **1** as a function of concentration. The straight lines represent the calculated fit of the experimental data points.

since the amide hydrogens may exhibit cross-peaks with either the H-2 or H-4(6) protons of the isophthalic ring depending on whether the rotameric form present corresponds to the helical or to the "linear" geometries, respectively. It would have been desirable to compare the NOE correlations for the receptor **1** in the presence and absence of the cyanurate template **4**. However, due to the aforementioned nonspecific self-aggregation of compound **1** in $CDCl_3$, no NOE spectrum could be measured for **1** in the absence of template and so a suitable model system was sought. Compound **3c**, a truncated analogue of **1**, proved to be useful in this regard. The $^1$H NOE spectrum of **3c** in the absence of template **4** at 0.5 mM concentration showed two cross peaks of equal intensity for the isophthaloyl amide protons with the H-2 and H-4(6) protons of the isophthalic ring, indicating that there was no preference for any of the three possible rotameric forms. Upon introduction of one equivalent or more of **4**, the amide protons gave only one cross-peak with the H-2 proton of the isophthaloyl moiety, thus demonstrating a binding induced shift in the rotameric equilibria towards the curved species. Similarly, the oligoisophthalamide **1** itself, upon treatment with two equivalents of cyanurate, displayed three major cross-peaks for three of the four amide hydrogens: $NH_A$ with H-2 and both $NH_B$ and $NH_C$ with H-2′. Additionally, three minor cross-peaks for three of the four amide hydrogens, $NH_A$ with H-4, $NH_B$ with H-4′ and $NH_C$ with H-6′ were observed. A comparison of the relative intensities of the NOE cross-peaks suggests that the predominant species formed in solution by **1:4**$_2$ (Figure 9) is of helical nature. The helix is apparently more stable than the S-shaped and C-shaped conformers, possibly because of intramolecular stacking interactions within the helix.

For the reasons described above, no information about the rotameric equilibria could be obtained from the NOE spectrum for **1** (5 mM) saturated with four equivalents of the naphthalimide template.

**Second level assembly into fiber structures**: We have shown that intermolecular H-bonding between **1** and **4** leads to helical discrete architectures at low concentrations. Upon increasing concentration, further aggregation may be expected for such structures containing flat aromatic units, generating eventually fibrous columnar entities as observed for other systems reported in the literature.[21] We sought for such stacked structures by increasing concentration and decreasing solvent polarity. Thus, the $^1$H NMR signals of a solution of **1:4**$_2$ in $CDCl_3$ and especially those in the aromatic region shift upfield when increasing concentration from 0.125 to 40 mM (up to 0.2 ppm), or upon successive addition of deuterated cyclohexane $C_6D_{12}$ up to 60% to a 5 mM solution of **1:4**$_2$ complex in $CDCl_3$ (up to 0.18 ppm), despite the dilution which was previously shown to favor the opposite trend.

This suggests that further aggregation indeed takes place under these conditions. More specifically, upfield shifts were interpreted as the consequence of face to face stacking interactions within oligomeric species of variable sizes. The signals remain sharp indicating that exchange occurs rapidly on the NMR time scale.

In an attempt to determine whether these aggregates do correspond to incremental additions of a monomer to an oligomer with expectably identical free energies, we performed a quantitative analysis of the stepwise dilution of the **1:4**$_2$ complex from 40 mM down to 0.125 mM. For this, we followed several aromatic NMR signal shifts and assumed, on the basis of the high association constants, the presence of a

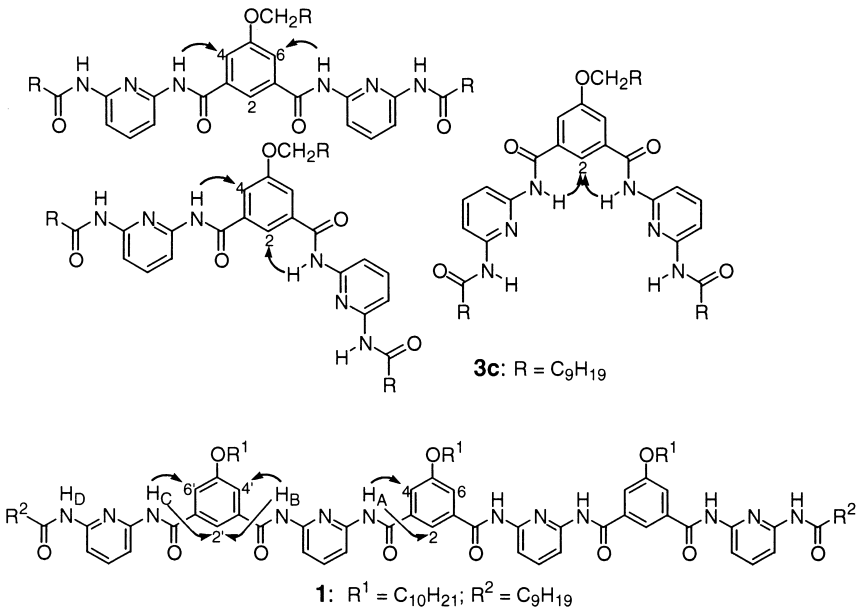


Figure 9. Top: possible rotameric forms of the oligo-amides **3c** and possible NOE cross correlations. Bottom: observed NOE correlations for **1:4**$_2$.

single (predominant) species **1:4**$_2$ in solution within the whole concentration range. All possible conformers were assumed to aggregate with similar constants.

The chemical shift values of three aromatic protons as a function of complex concentration were used as input for the Chem-Equili program. All data sets fit very well a simple dimerization event according to Equation (3), with log $K_{dim}$ = 1.88(0.03), a value which is close to those reported for comparable systems.[24]

$$K_{dim}: 2(\mathbf{1}:\mathbf{4}) \rightleftharpoons (\mathbf{1}:\mathbf{4}_2)_2 \quad (3)$$

Good fits are also obtained when taking into account the formation of trimers and higher order aggregates. However, the values for the successive association constants are given with large error margins to indicate that the dilution data have low information content for their determination. Most likely, the formation of these higher order aggregates is not sufficient within the concentration range studied to affect significantly the shape of the dilution curve (Figure 10).

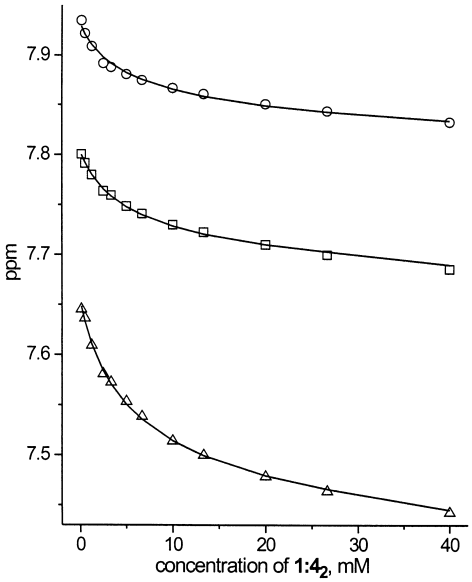


Figure 10. Variation of the chemical shift of three selected aromatic proton NMR signals of **1** on the **1:4**$_2$ complex on dilution in $CDCl_3$. The curves represent the calculated fit for the indicated binding constant of the dimerization.

However, it is not clear whether stacking in solution occurs directly between the helical conformers of **1:4**$_2$ observed at low concentration, or whether it also involves S-shaped and C-shaped conformers. Indeed, NOE experiments performed at 5 mM show the expected two cross peaks of $NH_B$ and $NH_C$ both with H-2′ with no traces of cross peaks of $NH_B$ with H-4′ and of $NH_C$ with H-6′, but unlike the results obtained at lower concentration (0.5 mM), $NH_A$ shows two cross peaks of nearly equal intensity with H-2 and H-4, consistent with the existence of C-shaped and S-shaped conformers, in addition to the helical one. This could indicate that at higher concentration there is an increase in the fraction of forms in which the template is bound less strongly and/or which polyassociate more weakly, such as the linear entity BLF (Figure 3). However any interpretation can only be very tentative in view of the complexity of the process and the variety of possible species.

Definite evidence of second level aggregation of **1:4**$_2$ complexes was obtained after noting that addition of a hydrocarbon solvent such as cyclohexane or tetradecane to a 20–40 mM chloroform solution results in a strong viscoelasticity, consistent with the formation of long and entangled fibers. In the same solvent conditions, **1** or **4** alone simply precipitate. Under crossed-polarizers, the viscous solutions did not show any particular texture. However, shearing of the solution by simple vigorous stirring resulted in birefringence which was interpreted as a trace of fiber alignment under shear.

These observations prompted us to examine these viscous solutions by electron microscopy (EM).

**Electron microscopy analysis**: The viscous solutions of **1:4**$_2$ were investigated by electron microscopy (EM). As the solutions in $CHCl_3$/hexane were evaporating too quickly on the grid, coating the whole surface with material, we used higher boiling $C_2H_2Cl_4$ and mixtures of $C_2H_2Cl_4$ with heptane as solvents. The dilute solution (2–10 mM) of **1:4**$_2$ in pure tetrachloroethane were analyzed by spreading on a carbon supporting film and rotary shadowing. For all concentrations (1–10 mM), the formation of fibers was observed. The fibers are up to 1 μm in length and 47–75 Å in diameter and show a clear natural tendency to aggregate and to form larger bundles and two-dimensional sheets with a periodicity of 113–117 Å (Figure 11a). The fibers present no internal helicity and tend to be straight with a high persistence length. Preliminary analyses by cryo electron microscopy (data not shown) allowed to determine more precisely the diameter of

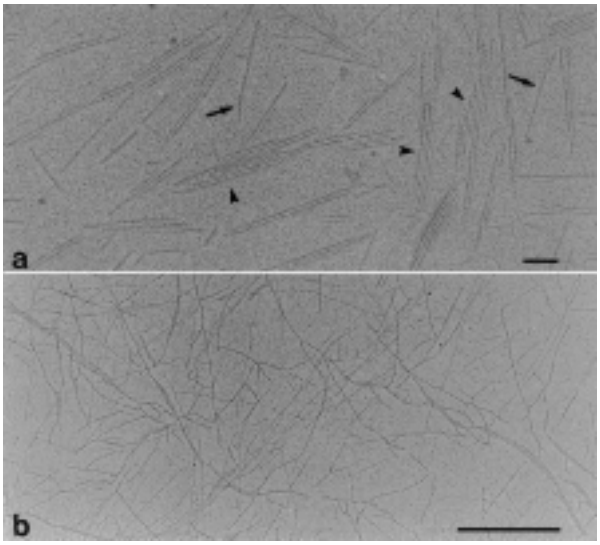


Figure 11. a) 5 mM solution of **1:4**$_2$ in pure $C_2H_2Cl_4$, observed after adsorption on a carbon film and rotary showing. Fibers are observed with a diameter of 47–75 Å (arrows), that often assemble to form 2D sheets (arrowheads) (bar 1000 Å). b) 2 mM solution of **1:4**$_2$ in $C_2H_2Cl_4$/heptane 1:9. Very long entangled fibers are observed. They form larger bundles up to several μm in length (bar 1 μm).



0947-6539/00/0611-1944 $ 17.50+.50/0 *Chem. Eur. J.* **2000**, *6*, No. 11

the fibers in the frozen-solvated state to be around 50 Å. This value is close to the calculated diameter of 43 Å of the **1:4**$_2$ helical disklike object (Figure 3), assuming radially protruding and linearly disposed alkoxy chains. However, it does not exclude the presence of linear forms such as BLF (Figure 3). The structural analysis by the cryoEM technique is being pursued.

Diluting the pure $C_2H_2Cl_4$ solutions with heptane (up to 90%) results in the formation of much longer fibers of several microns of length (measured from 3–6 μm) of a similar diameter range as observed for the fibers obtained from the pure $C_2H_2Cl_4$ solutions. The fibers are randomly disordered and show a high degree of entanglement, which explains the macroscopic observation of the formation of a visco-elastic solution, as previously described (Figure 11b).

In the numerous control experiments performed on the pure components **1** and **4** no fibers were observed under various conditions similar to or different from those under which they were observed for the **1:4**$_2$ mixture.

One may point out that the formation of extended fibers as described above, represents a template-induced hierarchical self-assembly process: the binding of the two cyanurate units leads to an entity **1**:**4**$_2$ which sets the stage for the subsequent polyassociation into fibers. On another line, it is worth noting that a hierarchical self-assembly process amounts also to an IF logic function (and a case of conditional probability), the second stage being accessible only *if* the first one is realized.

## Conclusion

The incorporation of specific H-bonding arrays into the components sets the stage for the design of recognition capable materials. The utilization of template direction in the assembly process contributes even greater capabilities by facilitating tandem-hierarchical self-organization events and allowing the interactional algorithm to be read in different ways. It has been shown that the reading of the same ligand information through different metal ion coordination algorithms generates different output species, amounting to a multiple processing behavior.[16–18] In the present system multiple reading takes place through different H-bonding based interactional schemes. Receptor **1** can in principle be read out linearly upon interaction with an imide template, or may bind a cyanurate effector, to form a disklike object, which itself undergoes a subsequent self-organization event: aggregation to form columnar structures. Furthermore, an additional means of control is represented by the medium, that is fiber formation depends critically on the solvent composition, temperature and concentration. The ability to identify and selectively orchestrate the interactional features governing the outcome of competitive self-assembly processes makes possible the expression of a specific member of a dynamic structural/conformational library.[15, 25] The dependence on medium effects confers adaptive character to the material. Such features, dynamic diversity[25] and adaptability[17] open novel perspectives to materials science.

## Experimental Section

**General methods**: THF was distilled over sodium/benzophenone. Triethylamine (Lancaster, 99%) was used as received. Flash column chromatography was performed using silica gel (Geduran, SI 60 (40–63 mm, Merck). Infrared spectra were recorded as thin films on NaCl discs on a Perkin Elmer 1600 Series FTIR. 500 MHz $^1$H NOESY spectra were recorded on a Bruker ARX 500 spectrometer, 300 MHz $^1$H NMR and and 75 MHz $^{13}$C NMR spectra on a Bruker AM 300 spectrometer, and 200 MHz $^1$H NMR and 50 MHz $^{13}$C NMR spectra on a Bruker SY 200 spectrometer. The solvent signal was used as an internal reference for both $^1$H and $^{13}$C NMR spectra. The following notation is used for the $^1$H NMR spectral splitting patterns: singlet (s), doublet (d), triplet (t), multiplet (m). EI and FAB mass spectrometric measurements were performed by the Service de Spectrométrie de Masse, Institut de Chimie, Université Louis Pasteur. Melting points (m.p.) were recorded on an electrothermal Digital Melting Point Apparatus and are uncorrected. Elemental analyses were performed by the Service de Microanalyse, Institut de Chimie, Université Louis Pasteur.

**Electron microscopy**: A 2 to 10 mM solution of **1:4**$_2$ (5 μL) in the different solvents was deposited on to a 400 mesh EM grid covered with a carbon supporting film. The solution was adsorbed (2 min) and the excess of solution was removed with a piece of filter paper (Whatmann 2 or 5) and air dried. The grids were then put in an Auto 306 evaporator (Edwards) and rotary shadowed at an angle of 13° with platinum/tungsten. The grids were then observed in a Philips CM12 electron microscope operating at 100 kV.

**Dimethyl 5-decyloxy-isophthalate (2a), *N,N′*-bis-(6-amino-pyridin-2-yl)-5-decyloxy-isophthalamide (3a), and *N,N′*-bis-(6-decanoylaminopyridin-2-yl)-5-decyloxy-isophthalamide (3c)**: known compounds prepared according to literature procedures.[25]

**5-Decyloxy-isophthalic acid (2b)**: **2a** (5.88 g, 16.7 mmol, 100 mol%) was dissolved in ethanol (167 mL) at 65 °C and a 1M solution of NaOH in water (2.68 g, 67 mmol, 400 mol%, in 16 mL $H_2O$) was added. The mixture was stirred at 65 °C for 8 h, cooled to room temperature, and filtered. The residue was washed with diethyl ether and dissolved in water. The solution was acidified with concentrated HCl, and the precipitate was collected by filtration and dried under high vacuum. The title compound **2b** was obtained as a white powder (5.1 g, 95%). M.p. 213–214 °C. IR (thin film): $\tilde{\nu}$ = 2922, 1709, 1595, 1411, 1272, 1047, 761, 733 cm$^{-1}$; $^1$H NMR (200 MHz, [D$_6$]DMSO): $\delta$ = 8.06 (t, $J$ = 1.4 Hz, 1H), 7.62 (d, $J$ = 1.4 Hz, 2H), 4.06 (t, $J$ = 6.4 Hz, 2H), 1.72 (m, 2H), 1.23 (m, 14H), 0.84 (t, $J$ = 6.4 Hz, 3H); $^{13}$C NMR (50 MHz, [D$_6$]DMSO): $\delta$ = 166.3, 158.7, 132.5, 122.0, 118.9, 68.0, 31.2, 28.8, 28.6, 28.4, 25.3, 22.0, 13.8; FAB-MS: $m/z$: 321.3 ([$M$ – H]$^-$, 100%); HRMS (FAB-MS) calcd. for $C_{18}H_{26}O_5$ 322.1780, found 322.1787.

***N*-(6-Aminopyridin-2-yl)-*N′*-(6-decanyolaminopyridin-2-yl)-5-decyloxy-isophthalamide (3b)**: To a solution of **3a** (7.80 g, 15.5 mmol, 100 mol%) and triethylamine (0.79 g, 7.7 mmol, 50 mol%) in dry THF (40 mL) was added dropwise a solution of decanoyl chloride (1.47 g, 7.7 mmol, 50 mol%) in THF (8 mL) at 0 °C and the reaction stirred for 1 h, before warming to room temperature. The reaction mixture was filtered, evaporated to dryness and applied to a column ($SiO_2$; EtOAc/hexane 1:3) to provide **3b** (3.2 g, 32% yield). Under these conditions, the amount of undesired side product **3c** (0.7 g, 6%) was small and the unreacted starting material **3a** (4.1 g, 53%) was recovered. **3b**: White powder. M.p. 93–94 °C. IR (thin film): $\tilde{\nu}$ = 3316, 2925, 2864, 1678, 1585, 1520, 1449, 1299, 1292, 1243, 1155, 1049, 881, 793, 721 cm$^{-1}$; $^1$H NMR (300 MHz, $CDCl_3$): $\delta$ = 9.51 (br. s, 1H), 8.74 (br. s, 1H), 8.72 (br. s, 1H), 7.87 (m, 3H), 7.55 (m, 4H), 7.44 (t, $^3J$ = 8.0 Hz, 1H), 6.13 (d, $^3J$ = 8.0 Hz, 1H), 4.55 (br. s, 2H), 3.86 (t, $^3J$ = 6.5 Hz, 2H), 2.40 (t, $^3J$ = 7.5 Hz, 2H), 1.67 (m, 4H), 1.24 (m, 26H), 0.83 (m, 6H); $^{13}$C NMR (75 MHz, $CDCl_3$): $\delta$ = 172.4, 165.0, 164.3, 159.7, 149.9, 149.6, 149.2, 140.4, 140.1, 135.7, 135.4, 117.6, 117.3, 116.9, 109.9, 109.5, 105.0, 104.0, 68.5, 37.4, 31.8, 29.5, 29.3, 29.2, 29.0, 25.9, 25.3, 23.6, 22.6, 14.0; FAB-MS: $m/z$: 659.4 ([$M$+H]$^+$, 100%); elemental analysis calc. (%) for $C_{38}H_{54}N_6O_4$ (658.88): C 69.27, H 8.26; found: C 69.30, H 8.28.

***N,N′*-Bis-(6-{[6-(6-decanoylamino-pyridin-2-ylcarbamoyl)-4-decyloxy-benzoylamino]-pyridin-2-yl}-5-decyloxy-isophthalamide (1)**: The diacid **2b** (0.95 g, 2.86 mmol, 124 mol%) was suspended in $SOCl_2$ (20 mL) and heated to reflux for 5 h after which time $SOCl_2$ was distilled off. The remaining oily isophthaloyl chloride **2c** was dried under high vacuum, dissolved in dry THF (3 mL) and immediately transferred by syringe to a

previously prepared solution of mono-amine **3b** (3.0 g, 4.55 mmol, 200 mol%) and triethylamine (0.47 g, 4.7 mmol, 206 mol%) in dry THF (15 mL) at 0 °C. The reaction was monitored by TLC (eluent: 1% MeOH/$CH_2Cl_2$). Compound **2c** (112 mol%) was added at which point **3b** was completely consumed. The reaction mixture was then filtered, evaporated to dryness, and the residue was purified by column chromatography ($SiO_2$; slow gradient 1% MeOH/$CH_2Cl_2$ to 3% MeOH/$CH_2Cl_2$). The collected fractions were evaporated to about 20 mL, diethyl ether was added (50 mL), the precipitate was filtered and dried under high vacuum. Isophthalamide **1** was obtained as a slightly yellow powder (2.71 g, 74%). M.p. 110–111 °C. IR (thin film): $\tilde{\nu}$ = 3304, 2925, 2854, 1682, 1586, 1520, 1448, 1402, 1315, 1243, 1156, 1121, 1051, 993, 881, 797, 739, 739 $cm^{-1}$; $^1H$ NMR (500 MHz, $CDCl_3$, 0.5 mM): $\delta$ = 8.98 (br. s, 2H), 8.52 (br. m, 4H), 8.18 (br. m, 1H), 8.11 (br. m, 2H), 8.02 (br. m, 2H), 7.89 (br. m, 6H), 7.77 (br. m, 4H), 7.66 (br. t, $^3J$ = 8.0 Hz, 4H), 7.57 (br. m, 2H), 7.53 (br. m, 2H), 4.05 (br. t, $^3J$ = 6.5 Hz, 2H), 3.94 (br. t, $^3J$ = 6.3 Hz, 4H), 2.25 (br. t, $^3J$ = 6.5 Hz, 4H), 1.80 (br. m, 2H), 1.74 (br. m, 4H), 1.28 (m, 66H), 0.83 (m, 15H); $^{13}C$ NMR (125 MHz, $CDCl_3$, 0.5 mM): $\delta$ = 172.49, 165.09, 165.06, 159.86, 159.36, 151.77, 150.62, 150.41, 150.04, 149.97, 149.40, 147.98, 140.90, 135.29, 134.92, 118.54, 118.12, 118.01, 116.09, 112.69, 112.54, 111.75, 111.31, 68.59, 37.14, 31.87, 31.85, 29.62, 29.61, 29.59, 29.55, 29.49, 29.48, 29.40, 29.33, 29.07, 26.64, 26.06, 25.93, 25.25, 22.67, 22.65, 14.18, 14.08; FAB-MS: *m/z*: 1604.0 ([$M^+$], 60%); elemental analysis calcd (%) for $C_{94}H_{130}N_{12}O_{11}$ (1604.14): C 70.38, H 8.17; found: C 70.37, H 8.26.

**1** in complex **1:4**$_2$: $^1H$ NMR (500 MHz, $CDCl_3$, 0.5 mM): $\delta$ = 9.54 (br. s, 2H), 9.38 (br. s, 2H), 9.20 (br. s, 2H), 8.68 (br. s, 2H), 8.10 (d, $^3J$ = 7.8 Hz, 2H), 8.08 (d, $^3J$ = 7.8 Hz, 2H), 8.02 (s, 1H), 8.01 (d, $^3J$ = 8.0 Hz, 2H), 7.98 (s, 2H), 7.94 (d, $^3J$ = 8.5 Hz, 2H), 7.89 (t, $^3J$ = 8.3 Hz, 2H), 7.75 (t, $^3J$ = 8.2 Hz, 2H), 7.71 (s, 2H), 7.64 (s, 2H), 7.62 (s, 2H), 4.09 (t, $^3J$ = 6.7 Hz, 2H), 4.01 (t, $^3J$ = 6.6 Hz, 4H), 2.33 (t, $^3J$ = 7.3 Hz, 4H), 1.83 (m, 2H), 1.78 (m, 4H), 1.68 (m, 4H), 1.27 (m, 66H), 0.87 (m, 15H). **4** in complex **1:4**$_2$: $^1H$-NMR (500 MHz, $CDCl_3$, 0.5 mM): $\delta$ = 12.32 (br. s, 4H), 3.75 (t, $^3J$ = 7.5 Hz, 4H), 1.44 (m, 4H), 1.17 (m, 14H), 0.85 (m, 6H).

**1-Decyl-[1,3,5]triazinane-2,4,6-trione 4 (decyl cyanurate)**: A solution of [1,3,5]triazinane-2,4,6-trione (cyanuric acid) (5.16 g, 40 mmol, 200 mol%), decyl bromide (4.14 mL, 20 mmol, 100 mol%), and $K_2CO_3$ (2.76 g, 20 mmol, 100 mol%) in DMSO (40 mL) was stirred at 60 °C for 22 h. The reaction mixture was partitioned between diethyl ether and saturated $NaHSO_{4(aq)}$. The organic phase was washed three times with brine, dried over $Na_2SO_4$, filtered, and evaporated to approximately 50 mL. Hexane was added dropwise with stirring, the resulting precipitate was collected by vacuum filtration and dried under high vacuum to yield decyl cyanurate **4** as a white powder (2.9 g, 27%). M.p. 181–182 °C. IR (thin film): $\tilde{\nu}$ = 3200, 2910, 2844, 1740, 1660, 1442 $cm^{-1}$; $^1H$ NMR (200 MHz, [$D_6$]DMSO): $\delta$ = 9.22 (br. s, 2H), 3.61 (t, $^3J$ = 7.1 Hz, 2H), 1.49 (m, 2H), 1.23 (m, 14H), 0.84 (t, $^3J$ = 6.4 Hz, 3H); $^{13}C$ NMR (50 MHz, [$D_6$]DMSO): $\delta$ = 149.7, 148.5, 31.2, 28.8, 28.6, 27.2, 26.0, 22.0, 13.8. FAB-MS: *m/z*: 270.1 ([$M$+H]$^+$, 85%); elemental analysis calc. (%) for $C_{13}H_{23}N_3O_3$ (269.34): C 57.97, H 8,61; found: C 57.86, H 8.46.

## Acknowledgement

This work was supported by the CNRS and by a predoctoral fellowship (V. B.) from the Forschungszentrum Karlsruhe GmbH. M. S. is supported by the "Institut National de la Santé et de la Recherche Médicale, le Centre National de la Recherche Scientifique et l'Hôpital Universitaire de Strasbourg".

[1] J.-M. Lehn, *Makromol. Chem. Macromol. Symp.* **1993**, *69*, 1.
[2] For a review see: Y. Xia, G. M. Whitesides, *Angew. Chem.* **1998**, *110*, 568; *Angew. Chem. Int. Ed.* **1998**, *37*, 550.
[3] a) J.-M. Lehn, *Angew. Chem.* **1990**, *102*, 1347–1362; *Angew. Chem. Int. Ed. Engl.* **1990**, *29*, 1304; b) J.-M. Lehn, *Supramolecular Chemistry: Concepts and Perspectives*, VCH, Weinheim, **1995**, Chap. 9.
[4] G. M. Whitesides, J. P. Matthias, C. T. Seto, *Science* **1991**, *254*, 1312.
[5] D. Philp, J. F. Stoddart, *Angew. Chem.* **1996**, *108*, 1242; *Angew. Chem. Int. Ed. Engl.* **1996**, *35*, 1154.
[6] a) M. Etter, *Acc. Chem. Res.* **1990**, *23*, 120; b) D. S. Lawrence, T. Jiang, M. Levett, *Chem. Rev.* **1995**, *95*, 2229; c) V. A. Russel, W. D. Ward, *Chem. Mater.* **1996**, *8*, 1654; d) G. R. Desiraju, C. V. K. Sharma, "Crystal engineering and molecular recognition. Twin facets of supramolecular chemistry" in *Perspectives in Supramolecular Chemistry*, *Vol. 2: The Crystal as a Supramolecular Entity* (Ed.: G. R. Desiraju), Wiley, Chichester, **1995**.
[7] M. J. Krische, J.-M. Lehn, *Struct. Bonding* **1999**, in press.
[8] M.-J. Brienne, J. Gabard, J.-M. Lehn, I. Stibor, *J. Chem. Soc. Chem. Commun.* **1989**, 1868.
[9] a) C. Fouquey, J.-M. Lehn, *Adv. Mater.* **1990**, *2*, 254; b) T. Gulik-Krzywicki, C. Fouquey, J.-M. Lehn, *Proc. Natl. Acad. Sci. USA* **1993**, *90*, 163; c) M. Kotera, J.-M. Lehn, J.-P. Vigneron, *J. Chem. Soc. Chem. Commun.* **1994**, 197.
[10] F. S. Schoonbeek, J. H. van Esch, B. Wegewijs, D. B. A. Rep, M. P. de Haas, T. M. Klapwijk, R. M. Kellogg, B. L. Feringa, *Angew. Chem.* **1999**, *111*, 1486; *Angew. Chem. Int. Ed.* **1999**, *38*, 1393.
[11] D. Papoutsakis, J. P. Kirby, J. E. Jackson, D. G. Nocera, *Chem. Eur. J.* **1999**, 5, 1474.
[12] a) D. M. Bassani, J.-M. Lehn, G. Baum, D. Fenske, *Angew. Chem.* **1997**, *109*, 1931; *Angew. Chem. Int. Ed. Engl.* **1997**, *36*, 1845; b) A. E. Rowan, R. J. M. Nolte, *Angew. Chem.* **1998**, *110*, 65; *Angew. Chem. Int. Ed.* **1998**, *37*, 63; c) M. Ohkita, J.-M. Lehn, G. Baum, D. Fenske, *Chem. Eur. J.* **1999**, *5*, 3471.
[13] L. Cuccia, J.-M. Lehn, J.-C. Homo, M. Schmutz, *Angew. Chem.* **2000**, *112*, 239; *Angew. Chem. Int. Ed.* **2000**, *39*, 233.
[14] M. Suárez, J.-M. Lehn, S. C. Zimmerman, A. Skoulios, B. Heinrich, *J. Am. Chem. Soc.* **1998**, *120*, 9526.
[15] J.-M. Lehn, *Chem. Eur. J.* **1999**, *5*, 2464, and references therein.
[16] V. Smith, J.-M. Lehn, *Chem. Commun.* **1996**, 2733.
[17] J.-M. Lehn in *Supramolecular Science: Where It Is and Where It Is Going* (Eds.: R. Ungaro, E. Dalcanale), **1999**, Kluwer, Dordrecht, p. 287 and Figure 4 therein.
[18] a) D. P. Funeriu, J.-M. Lehn, G. Baum, D. Fenske, *Chem Eur. J.* **1997**, *3*, 99; b) D. P. Funeriu, J.-M. Lehn, unpublished results; c) D. P. Funeriu, Thése de Doctorat, Université Louis Pasteur, Strasbourg, **1999**.
[19] S.-K. Chang, D. Van Engen, E. Fan, A. D. Hamilton, *J. Am. Chem. Soc.* **1991**, *113*, 7640.
[20] Molecular modeling was performed with the Macromodel (version 5.5) molecular mechanics program using the Amber* force field for energy minimization.S. J. Weiner, P. A. Kollman, D. Case, U. C. Singh, G. Alagona, S. Profeta, P. Weiner, *J. Am. Chem. Soc.* **1984**, *106*, 765.
[21] C. Nuckolls, T. J. Katz, G. Katz, P. J. Collings, L. Castellanos, *J. Am. Chem. Soc.* **1999**, *121*, 79 and references therein.
[22] a) M. T. Blanda, J. H. Horner, M. Newcomb, *J. Org. Chem.* **1989**, *54*, 4626; b) K. A. Connors, *Binding Constants, The Measurement of Molecular Complex Stability*, Wiley-Interscience, New York, **1987**, p. 24.
[23] CHEM-EQUILI is a computer program for the calculation of equilibrium constants and related values from many types of experimental data (IR, NMR, UV/Vis, and fluorescence spectrophotometry, potentiometry, calorimetry, conductometry, etc.). It is possible to use any combination of such kinds of methods simultaneously for reliable calculations of equilibrium constants. For a detailed description see: V. P. Solov'ev, E. A. Vnuk, N. N. Strakhova, O. A. Raevsky, "Thermodynamic of complexation of the macrocyclic polyethers with salts of alkali and alkaline-earth metals" VINITI, Moscow, **1991**. V. P. Solov'ev, V. E. Baulin, N. N. Strakhova, V. P. Kazachenko, V. K. Belsky, A. A. Varnek, T. A. Volkova, G. Wipff, *J. Chem. Soc. Perkin Trans. 2* **1998**, 1489.
[24] A. S. Shetty, J. Zhang, J. S. Moore, *J. Am. Chem. Soc.* **1996**, *118*, 1019.
[25] V. Berl, I. Huc, J.-M. Lehn, A. DeCian, J. Fischer, *Eur. J. Org. Chem.* **1999**, 3089.

Received: January 5, 2000 [F2225]

  0947-6539/00/0611-1946 $ 17.50+.50/0 